Toughness Enhancement in ROMP Functionalized Carbon Nanotube/Polydicyclopentadiene Composites

Wonje Jeong and M. R. Kessler*

Department of Materials Science and Engineering, Iowa State University, Ames, Iowa 50011

Received July 30, 2008. Revised Manuscript Received September 17, 2008

Norbornene-functionalized multiwalled carbon nanotube (MWNT)/dicyclopentadiene (DCPD) nanocomposites have been prepared by ring-opening metathesis polymerization (ROMP). Tensile toughness is shown to increase by more than 900% compared to neat polyDCPD by incorporating just 0.4 wt % functionalized MWNTs. Modest increases in modulus and strength were also observed with increasing nanotube loadings. The effect of norbornene grafted MWNTs on the polymerization kinetics of the resulting cross-linked polyDCPD network was evaluated by differential scanning calorimetry (DSC). The glass-transition temperatures of the composites are shown to increase with addition of functionalized MWNTs. Moreover, a decrease in damping behavior, as measured by dynamic mechanical analysis, is used to estimate the effective polymer−particle interphase thickness.

Introduction

Since the first report of polymer nanocomposites using carbon nanotubes (CNTs) as filler in an epoxy matrix in the mid 1990s,[1] much interest has been shown by researchers within the polymer composites field. The high strength, modulus, and large aspect ratios of CNTs combined with their unmatched electrical and thermal properties make nanotubes attractive candidates for multifunctional nano-reinforced polymer composites.[2] However, their nonreactive surfaces and strong aggregative properties have limited the effectiveness of CNTs with the polymer matrices they reinforce. If the unique multifunctional properties of CNTs are to be utilized for effective reinforcement, well-dispersed nanotubes with good interfacial stress transfer with the polymer matrix is a prerequisite.[3] A number of surface-functionalization techniques have been proposed to tailor the nanotube surface for optimized compatibility with the polymer matrix. There are two main strategies for covalently functionalizing the nanotubes: the "grafting to" approach, which involves coupling of growing polymer molecules with reactive end groups to functional groups on the nanotube surface,[4] and the "grafting from" approach, which propagates reactions from initiation sites or reactive groups covalently attached on the nanotube surface.[5]

With the recent development of ruthenium-based catalysts (Grubbs catalysts) which are tolerant of a wide range of polar functionalities, ring-opening metathesis polymerization (ROMP) has recently emerged as a powerful tool to synthesize well-defined macromolecular materials.[6] ROMP also has been developed for synthetic protocols for the modification of inorganic surfaces such as silica,[7] silicon,[8] and gold;[9] both "grafting from" and "grafting to" approaches are applied to polymerize to and from the surface.

ROMP is also important for the production of industrially applicable polymers, the most important being polydicyclopentadiene (polyDCPD). PolyDCPD is a cross-linked polymer with high modulus, excellent impact strength, and chemical resistance formed by ROMP of its bicyclic olefin monomer.[10] These features, along with its quality surface,

* To whom correspondence should be addressed. E-mail: mkessler@iastate.edu.

(1) Ajayan, P. M.; Stephan, O.; Colliex, C.; Trauth, D. *Science* **1994**, *265*, 1212–1214.

(2) Baughman, R. H.; Zakhidov, A. A.; Heer, W. A. *Science* **2002**, *297*, 787–792.

(3) (a) Coleman, J. N.; Khan, U.; Gun'ko, Y. K. *Adv. Mater.* **2006**, *18*, 689–706. (b) Coleman, J. N.; Khan, U.; Blau, W. J.; Gun'ko, Y. K. *Carbon* **2006**, *44*, 1624–1652.

(4) (a) Fu, K.; Huang, W.; Lin, Y.; Riddle, L. A.; Carroll, D. L.; Sun, Y. P. *Nano Lett.* **2001**, *1*, 439–441. (b) Lou, X.; Detrembleur, C.; Sciannamea, V.; Pagnoulle, C.; Jerome, R. *Polymer* **2004**, *45*, 6097–6102. (c) Blake, R.; Gun'ko, Y. K.; Coleman, J.; Cadek, M.; Fonseca, A.; Nagy, J. B.; Blau, W. J. *J. Am. Chem. Soc.* **2004**, *126*, 10226–10227.

(5) (a) Qin, S.; Qin, D.; Ford, W. T.; Resasco, D. E.; Herrera, J. E. *Macromolecules* **2004**, *37*, 752–757. (b) Hwang, G. L.; Shieh, Y.-T.; Hwang, K. C. *Adv. Funct. Mater.* **2004**, *14*, 487–491. (c) Xia, H.; Wang, Q.; Qiu, G. *Chem. Mater.* **2003**, *15*, 3879–3886. (d) Tong, X.; Liu, C.; Cheng, H.-M.; Zhao, H.; Yang, F.; Zhang, X. *J. Appl. Polym. Sci.* **2004**, *92*, 3697–3700.

(6) (a) Buchmeiser, M. R. *Chem. Rev.* **2000**, *100*, 1565–1604. (b) Rurstner, A. *Angew. Chem., Int. Ed.* **2000**, *39*, 3012–3043. (c) Calderon, N. *J. Macromol. Sci. Rev. Macromol. Chem.* **1972**, *7*, 105–159. (d) Novak, B. M.; Risse, W.; Grubbs, R. H. *Adv. Polym. Sci.* **1992**, *102*, 47–72. (e) Ivin, K. J.; Mol, J. C. *Olefin Metathesis and Metathesis Polymerization*; Academic Press: San Diego, 1997. (f) Frenzel, U.; Nuyken, O. *J. Polym. Sci., Part A: Polym. Chem.* **2002**, *40*, 2895–2916. (g) Grubbs, R. H. *Handbook of Metathesis*; Wiley-VCH: Weinheim, Germany, 2003; Vol. 3.

(7) Buchmeiser, M. R.; Sinner, F.; Mupa, M.; Wurst, K *Macromolecules* **2000**, *33*, 32–39.

(8) (a) Juang, A.; Scherman, O. A.; Grubbs, R. H.; Lewis, N. S. *Langmuir* **2001**, *17*, 1321–1323. (b) Harada, Y.; Girolami, G. S.; Nuzzo, R. G. *Langmuir* **2003**, *19*, 5104–5114.

(9) (a) Watson, K. J.; Zhu, J.; Nguyen, S. T.; Mirkin, C. A. *J. Am. Chem. Soc.* **1999**, *121*, 462–463. (b) Liu, X.; Guo, S.; Mirkin, C. A. *Angew. Chem.* **2003**, *115*, 4933–4937. (c) Weck, M.; Jackiw, J. J.; Rossi, R. R.; Weiss, P. S.; Grubbs, R. H *J. Am. Chem. Soc.* **1999**, *121*, 4088–4089. (d) Rutenberg, I. M.; Scherman, O. A.; Grubbs, R. H.; Jiang, W.; Garfunkel, E.; Bao, Z. *J. Am. Chem. Soc.* **2004**, *126*, 4062–4063.

10.1021/cm8020947 CCC: $40.75
Published on Web 10/28/2008

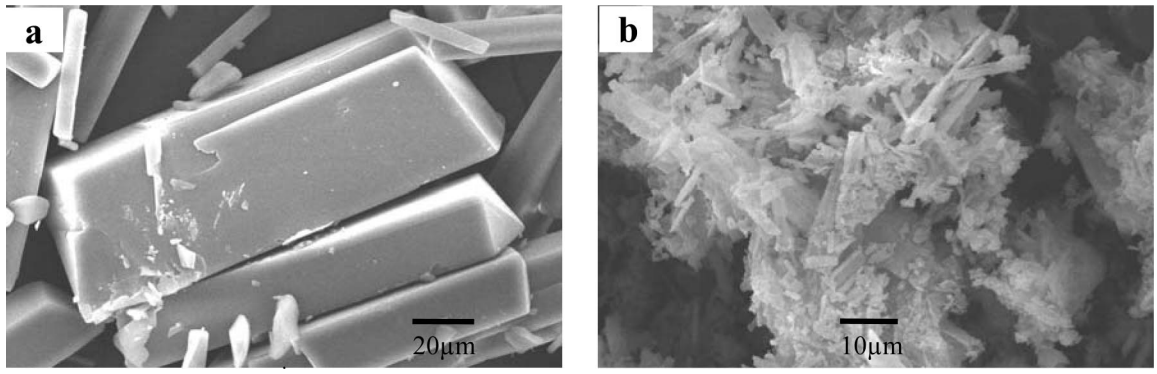

Figure 1. SEM of (a) as-supplied Grubbs' catalyst from Sigma-Aldrich, (b) recrystallized Grubbs' catalyst.

low cost, and processability, are leading to widespread use of polyDCPD in high-performance composite structures as a matrix material.[11] In order to use polyDCPD for a composite matrix the fillers need to be modified due to the highly nonpolar hydrophobic properties of DCPD. For example, Yoonessi et al. demonstrated that a high degree of nanoclay dispersion and partial exfoliation could be obtained using organically modified clay in a polyDCPD matrix processed through in situ ROMP.[12]

Recently, we have developed self-healing materials that autonomically repair microcrack damage in structural composites.[13] In these systems, microencapsulated DCPD monomer and Grubbs catalyst are embedded within an epoxy matrix. When the material is damaged, the microcapsules rupture and release the DCPD healing agent into the damage region where the healing agent contacts the catalyst, polymerization is initiated, and the damage is repaired. These self-healing composites possess great potential for mitigating microcracks and hidden damage, enabling structures with longer lifetimes and less maintenance. However, in order for this potential to be realized, the mechanical and adhesive strength of the ROMP-based healing agent system must be improved. Herein, with an ultimate goal of developing ROMP-based nanocomposite healing agents, we evaluate the effect of low loadings (<0.5 wt %) of CNTs on the mechanical properties of polyDCPD. High loadings of CNT reinforcements increase the viscosity of the liquid healing agents too dramatically, and are not considered in this work. The issue of dispersion, load transfer, and interfacial interactions is addressed by incorporation of norbornene-functionalized multiwalled nanotubes (f-MWNTs). We show that the use of f-MWNTs leads to improved interfacial interactions and physical properties through covalent "tethers" between the nanotube reinforcement and the polymer network.

Experimental Section

Materials. The MWNTs, produced by chemical vapor deposition (CVD) with O.D. × I.D. × length (15−20 nm × 5−10 nm × 0.5−200 μm, > 95%) and dichloro(3-methyl-2-butenylidine)bis-(tricyclopentyl)phosphine ruthenium (Grubbs' catalyst first Generation) were purchased from Aldrich Co. PTFE membrane filters (Pall Corporation) with an average pore size of 400 nm were used for all filtering steps. *N*,*N*′-Dimethylformamide (DMF), anhydrous ethylene glycol, and anhydrous pyridine were purchased from Aldrich and used without further purification. All other reagents and solvents were purchased from commercial suppliers and used as received. Both dicyclopentadiene (Alfa Aesar, 95+%) and 5-norbornene-2-yl(ethyl)chlorodimethylsilane (Hybrid Plastics) were also used as received. To improve the dispersion and interfacial adhesion of carbon nanotubes, we have developed a functionalization strategy where we first use acid-treated MWNTs to create −COOH-functionalized nanotubes and then attach norbornene moieties to the acid-functionalized nanotubes as described below.

Synthesis of MWNT-COOH. A two-step procedure was used to prepare the MWNT-COOH. First, as supplied MWNTs (1.1 g) and nitric acid (60%, 500 mL) were sonicated in an ultrasonic bath for 10 min to create an initial dispersion, followed by 6 h reflux at 130 °C. The filtered product was rinsed with DI water until neutral pH. Because nitric acid reflux produces carboxyl, hydroxyl, and carbonyl groups at the defect sites of the MWNTs, a second step of further oxidation with potassium permanganate solution in perchloric acid was performed to convert the hydroxyl and carbonyl groups to carboxyl groups using the procedure described by Sainsbury and Fitzmaurice[14] and by Kordas et al.[15] The final solution was filtered again and dried under vacuum at 100 °C for 24 h, giving MWNT-COOH (Scheme 1 (**1**)).

Synthesis of MWNT-Norbornene. The MWNT-COOH were refluxed in an excess of thionyl chloride with a catalytic amount of *N*,*N*′-Dimethylformamide (DMF) N_2 at 70 °C for 48 h. The residual $SOCl_2$ was removed by high vacuum distillation, giving acyl chloride-functionalized MWNTs (MWNT-COCl) (Scheme 1 (**2**)), which was immediately reacted with 40 mL of ethylene glycol and 0.1 mL of pyridine at 120 °C for 48 h, then purified. After being cooled, the solution was filtered and repeatedly rinsed with THF and acetone. The product was dried under a vacuum at 70 °C for 24 h, giving MWNT-OH (Scheme 1 (**3**)). The MWNT-OH was added in 5-norbornene-2-yl(ethyl)chlorodimethylsilane (25 mL) solution and 0.1 mL of pyridine and refluxed for 48 h at 70 °C.

(10) In *Encyclopedia of Chemical Technology*, 4th ed.; Howe Grant, M., Ed.; Wiley-Interscience: New York, 1996; Vol. 17, p 829.
(11) Woodson, C. S.; Grubbs, R. H. U.S. Patent 6 020 443, 2000.
(12) (a) Yoonessi, M.; Toghiani, H.; Kingery, W. L.; Pittman, C. U. *Macromolecules* **2004**, *37*, 2511–2518. (b) Yoonessi, M.; Toghiani, H.; Daulton, T. L.; Lin, J. S.; Pittman, C. U. *Macromolecules* **2005**, *38*, 818–831.
(13) (a) White, S. R.; Sottos, N. R.; Geubelle, P. H.; Moore, J. S.; Kessler, M. R.; Sriram, S. R.; Brown, E. N.; Viswanathan, S. *Nature* **2001**, *409*, 794–797. (b) Kessler, M. R.; Sottos, N. R.; White, S. R. *Composites, Part A* **2003**, *34*, 743–753. (c) Liu, X.; Lee, J. K.; Yoon, S. H.; Kessler, M. R. *J. Appl. Polym. Sci.* **2006**, *101*, 1266–1272.
(14) Sainsbury, T.; Fitzmaurice, D. *Chem. Mater.* **2004**, *16*, 2174–2179.
(15) Kordas, K.; Mustonen, T.; Toth, G.; Jantunen, H.; Lajunen, M.; Soldano, C.; Talapatra, S.; Kar, S.; Vajtai, R.; Ajayan, P. M. *Small* **2006**, *2*, 1021–1025.

Scheme 1

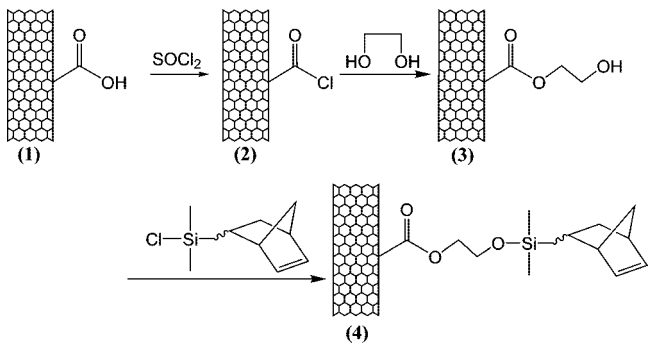

The solution was filtered and washed fully with THF and dried under a vacuum at 70 °C for 24 h, giving norbornene-functionalized MWNTs (Scheme 1(**4**)).

Preparation of Nanocomposites. Norbornene-functionalized MWNTs (f-MWNTs) were dispersed in DCPD by combining water bath and tip sonication. The crystal size and morphology of the Grubbs' catalyst affects its dissolution kinetics in the monomer.[16] To recrystallize the catalyst into a more soluble form, we first dissolved it in dichloromethane ($\sim 20 \times 10^{-3}$g/mL) and subjected it to dry nitrogen flow, forming a much smaller catalyst crystal morphology than the "as-received" catalyst (see Figure 1). The recrystallized catalyst was then mixed with the nanotube/DCPD solution (2.00×10^{-3}g of catalyst/1 mL of DCPD) to dissolve the catalyst powder, forming a homogeneous solution, followed by curing for 2 h at 70 °C and 1 h 30 min at 170 °C. All mechanical tests were done 1 day after sample preparation to minimize the effect of surface oxidation.[17] The weight percent was converted to volume fraction using eq 1:

$$V_f = \left[1 + \left(\frac{\rho_{NT}}{\rho_{pol}}\right)\left(\frac{1 - m_f}{m_f}\right)\right]^{-1} \quad (1)$$

where V_f and m_f are the volume fraction and weight fraction of the CNT filler respectively, and ρ_{NT} and ρ_{pol} are the density of CNTs and the polymer matrix respectively ($\rho_{NT}/\rho_{pol} = 2.2$).[18]

Characterization. Thermogravimetric analysis (TGA) was performed using a TA Instruments model Q50 TGA at a heating rate of 10 °C/min from room temperature to 850 °C with a continuous purge of air (40 mL/min). FTIR spectra were obtained from a Bruker Infared Spectrometer (IFS 66V/S). Samples were prepared as pellets using spectroscopic grade KBr. Differential scanning calorimetry (DSC) was performed using a TA Instruments model Q20 DSC. DCPD and f-MWNTs/DCPD solutions (0.2 and 0.4 wt %) were mixed with recrystallized Grubbs' catalyst and quenched dropwise into liquid nitrogen to create small frozen droplets of catalyzed solution, preventing premature cure at room temperature. Finally, the small frozen beads of catalyzed solution were placed into aluminum DSC sample pans and loaded into the DSC chamber at a standby temperature of −50 °C. The samples were scanned from −50 to 240 °C at a heating rate of 10 °C/min. Dynamic mechanical analysis (DMA) was performed using a TA Instruments model Q800 DMA. Samples were analyzed in tension mode at 1.0 Hz over a temperature range of 30 to 210 °C at a heating rate of 3 °C/min. The sample dimensions were 35 × 5 × 1 mm. The glass transition temperatures (T_g) were determined from the peak temperatures of the tan δ curves. Tension tests were performed with a Universal Testing Machine (Instron 5569) equipped with a noncontact video-extensometer on ASTM D638 type V samples at a crosshead speed of 1 mm/min. Each value reported is the average of at least four samples. The size distribution and dispersion status of f-MWNTs in the matrix were obtained by transmission electron microscopy (JEOL 1200EX). Samples of acid-treated and f-MWNTs were prepared by evaporating drops of nanotubes dispersed in *N*,*N*′-Dimethylformamide (DMF) solution

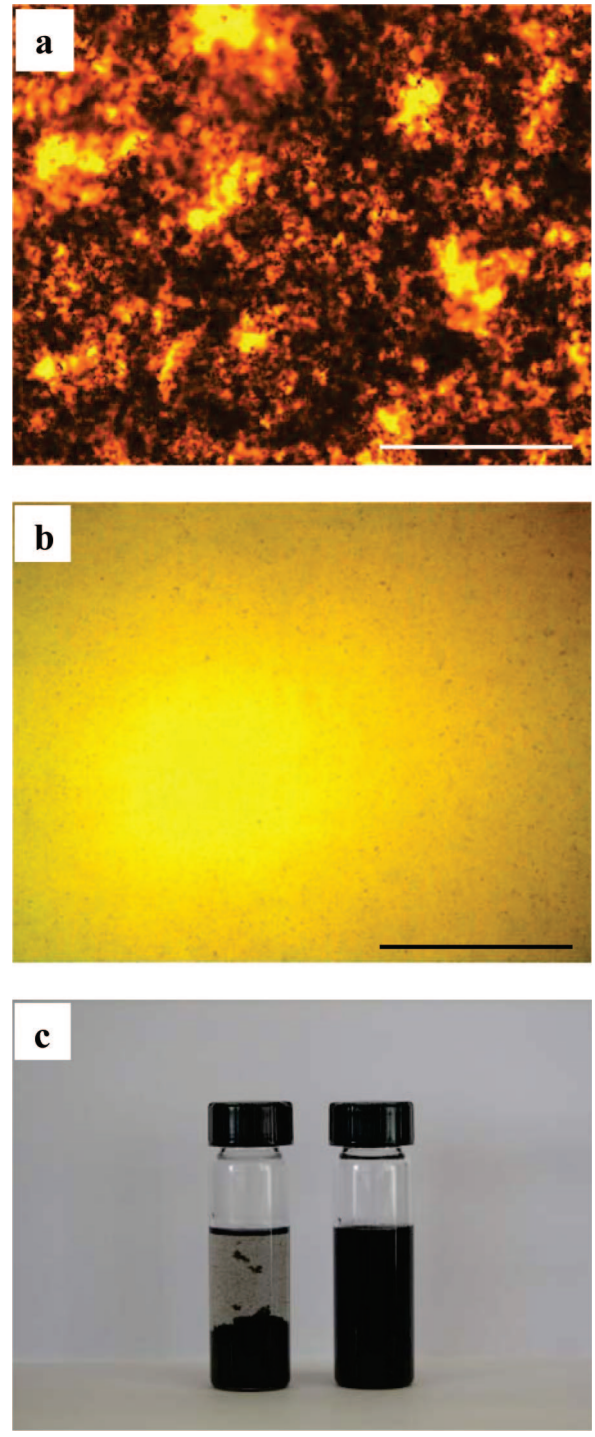

Figure 2. Optical microscopy images of the dispersion status of as supplied MWNTs (a) and norbornene-functionalized MWNTs (b) in DCPD solution (0.5 mg/mL scale bar = 1 mm) (c) Setting test of as-supplied and functionalized nanotubes in DCPD monomer (left, as-supplied MWNTs in DCPD monomer after 1 h; right, norborene-functionalized MWNTs in DCPD monomer after 1 day).

(16) Jones, A. S.; Rule, J. D.; Moore, J. S.; White, S. R.; Sottos, N. R. *Chem. Mater.* **2006**, *18*, 1312–1317.
(17) Kelsey, D. R.; Chuah, H. H.; Ellison, R. H.; Handlin, D. L.; Scardino, B. M. *J. Polym. Sci., Part A: Polym. Chem.* **1997**, *35*, 3049–3063.
(18) Blond, D.; Barron, V.; Ruether, M.; Ryan, K. P.; Nicolosi, V.; Blau, W. J.; Coleman, J. N. *Adv. Funct. Mater.* **2006**, *16*, 1608–1614.

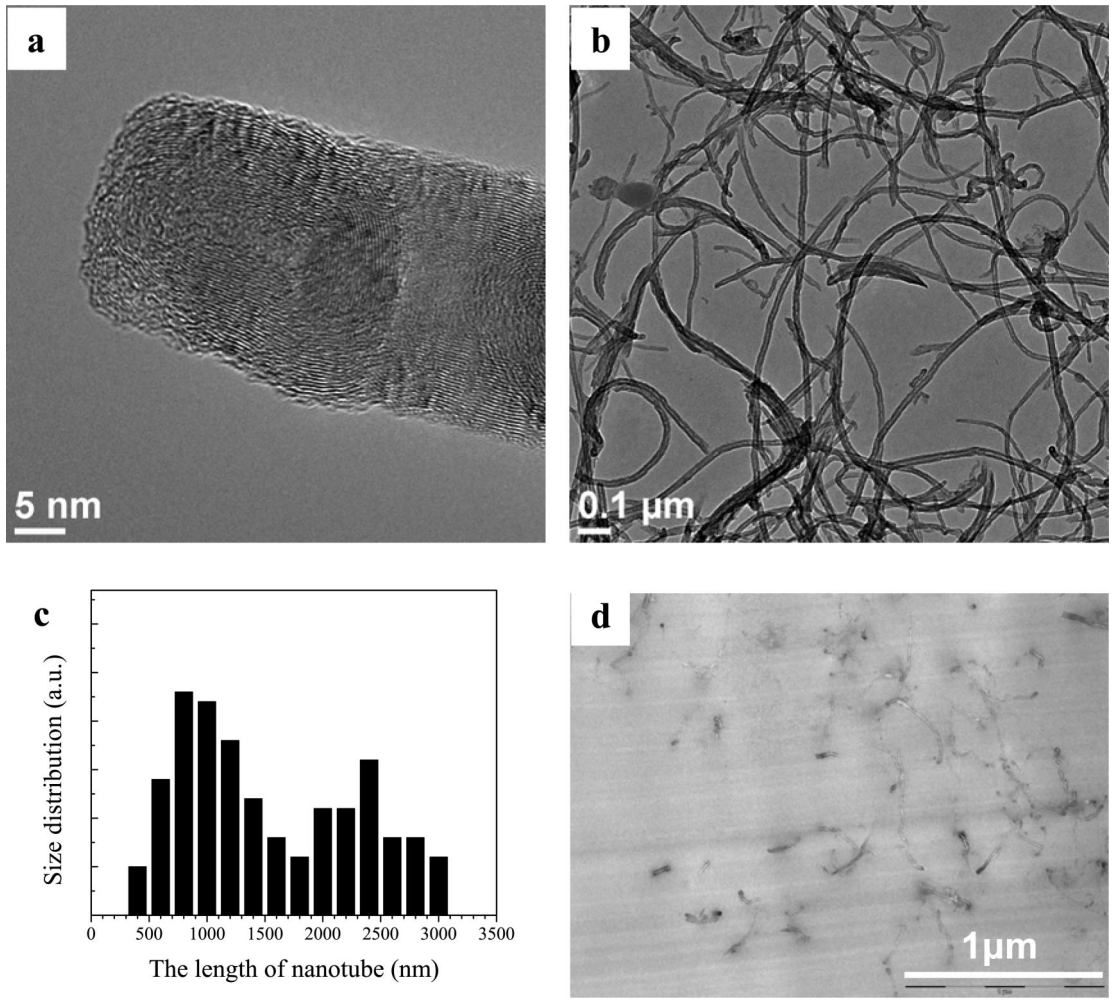

Figure 3. Transmission electron microscopy (TEM) images of (a) acid-treated MWNT, (b) norbornene-functionalized MWNT; (c) size-distribution plots of functionalized MWNT; (d) TEM image of norbornene-functionalized MWNT/polyDCPD composites.

on a carbon-coated copper grid. The composite was sliced into 70 nm thick sheets using an ultramicrotome for subsequent TEM analysis.

Results and Discussion

It was not possible to create well-dispersed suspensions of pristine nanotubes in DCPD monomer because of poor compatibility. As shown by optical microscopy (Figure 2a), when pristine MWNTs/DCPD suspensions are removed from the sonication bath, the nanotubes remain separate from the DCPD and form several hundred micrometer scale aggregations. To obtain uniform distribution in the monomer, we introduced norbornene grafted MWNTs using the procedures described above (see Experimental Section), with the expectation of improved compatibility between the nanotubes and the DCPD monomer. Optical microscopy shows that f-MWNTs are well-dispersed and homogeneously stable (Figure 2b). Figure 2c shows the dispersion of f-MWNTs (right) compared to 'as supplied' MWNTs (left) in DCPD monomer. The f-MWNTs are dispersed in DCPD easily once sonication starts and remain stable indefinitely, whereas "as-supplied" MWNTs agglomerate and settle to the bottom immediately following sonication. TEM images show that f-MWNTs have a broad length distribution, from submicrometer to 3 μm, which is shorter than expected, probably because of the harsh oxidation process and repeated sonication during functionalization (Figure 3).

Thermogravimetric analysis (TGA) was performed to verify the thermal stability of MWNT (Figure 4a). The oxidized MWNT-COOH decompose gradually with increasing temperature due to the decomposition of carboxyl groups on the surface of MWNT-COOH and show a higher decomposition onset temperature compared to pristine MWNTs because of the elimination of residue metal catalyst during acid treatment. The final weight for the "as-received" nanotubes is 7 wt %, corresponding to the residue metal catalyst used in CVD processing to form the nanotubes. For f-MWNTs, there is significant weight loss between 250 and 400 °C (onset is at 292 °C) that may be attributed to the decomposition of the norbornene moieties. The reduction of decomposition temperature for the f-MWNTs compared to MWNT-COOH may be attributed to the stronger surface interaction between the carboxyl groups of the acid treated nanotubes, which are much more closely packed together after drying in the vacuum oven. The increased weight loss may also be due to cleavage of weaker ether bonds or a retro Diels−Alder reaction possible in the f-MWNTs. The quantity of the norbornene moiety functionalized to the surface of the nanotubes is estimated from TGA as 16.85 wt % (at 480 °C).

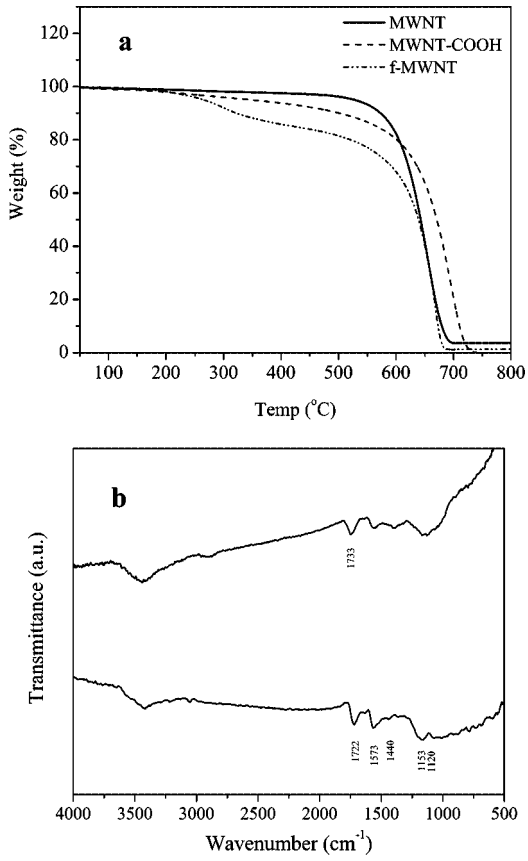

Figure 4. (a) Thermogravimetric analysis (TGA) weight loss curves of pristine, oxidized, and norbornene-functionalized MWNT; (b) FTIR spectra of acid-treated (top) and norbornene-functionalized MWNTs (bottom).

In the spectrum of acid-treated nanotubes (Figure 4b, top), the broad peak at 3100−3700 cm^{-1} is assigned to the O−H stretches of carboxyl groups. The peak at 1733 cm^{-1} corresponds to C═O stretch arising from the carboxylic acid groups. Figure 4b bottom shows the FTIR spectrum of f-MWNTs. The peak at 1722 cm^{-1} is similarly assigned to the C═O stretch of the ester, while peaks at 1573, 1120, 1153, and 1440 cm^{-1} correspond to C═C bonds of norbornene, O−Si stretch, C−O stretch of the ester group, and C−H bend of alkyl chains, respectively.

In order to make the MWNT/DCPD nanocomposites, the f-MWNTs/DCPD solution was mixed with recrystallized Grubbs' catalyst. Mixing DCPD with catalyst instantaneously initiates ROMP at room temperature. The catalyst opens the norbornyl double bond in DCPD, driven by ring strain relief, and a linear chain propagates. The remaining cyclopentenyl double bond can be polymerized in a similar way to form a cross-linked polyDCPD network.[19] Two different types of polymerization mechanisms between f-MWNTs and DCPD during ROMP are suggested. First propagating linear chains of DCPD encounter the norbornene moiety on the nanotube's surface and form covalent bonds in a "grafting to" approach (Scheme 2A). The other approach is that the norbornene moiety on the nanotube surface can be initiated by Grubbs' catalyst resulting in catalyst-functionalized nanotubes, where the front Ruthenium catalyst subsequently reacts with surrounding DCPD to form the nanotube-polyDCPD network

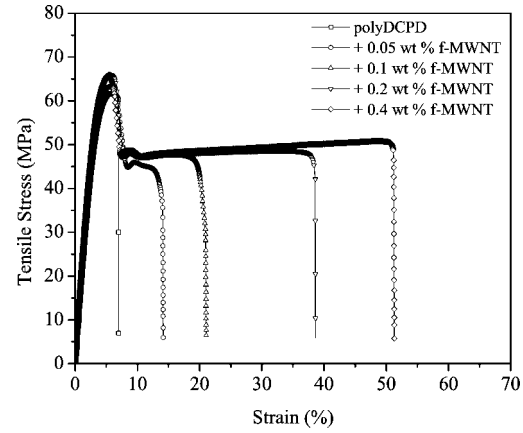

Figure 5. Representative stress−strain curves for norbornene-functionalized MWNT/polyDCPD composites with respect to nanotube weight percentage.

in a "grafting from" approach (Scheme 2B). Adronov et al. reported Grubbs' catalyst grafted single-walled carbon nanotubes using ROMP of norbornene and proposed that those functionalized catalysts on the surface of the nanotube can be used as rapid polymerization sites but bulk composites were not reported.[20] The second approach is kinetically favorable but statistically less likely because of the excess DCPD compared to f-MWNTs. With the combination of these two different mechanisms, covalent bonds between f-MWNTs and the polyDCPD are formed. These "tethers" between the nanotubes and the cross-linked network lead to improved interfacial stress transfer. Individual nanotubes are randomly dispersed throughout the matrix and no aggregation is observed by TEM observation of microtomed composite sections (Figure 3d). The scratched lines across the image in Figure 3d are due to microtome cutting.

Representative stress−strain curves for MWNT/polyDCPD nanocomposites with different f-MWNT loadings are shown in Figure 5. There is little increase in both Young's modulus and strength for the composites with increasing CNT loading; however, noticeable increases in elongation at break are observed. Neat polyDCPD shows "typical" brittle thermoset tensile behavior. When the material is loaded to its ultimate tensile strength, the specimen fractures quickly at an elongation of 5.75% (Figure 6a). In contrast, with increasing nanotube loading, when the material reaches its ultimate tensile strength, yielding occurs, and the sample extends further. Macroscopic changes were observed in the tensile specimens during extension. Above the yield point, the reinforced samples neck, with a local decrease in width within the gauge region. The width of the neck region remains constant as its length increases so there is no further reduction in cross-sectional area and the necking zone propagates along the gauge region until the sample finally breaks (Figure 6b). The elongation at break significantly increased from 5.75 to 51.8% with the addition of just 0.4 wt % f-MWNTs. Figure 6c shows the tensile specimens following fracture, exhibiting the necking in the gauge region and the fracture phenomena. Upon incorporation of only 0.4 wt % nanotubes, the tensile toughness (from the total area under the stress–strain curve) of the composites increased by 925% in a

(19) Fisher, R. A.; Grubbs, R. H. *Makromol. Chem. Macromol. Symp.* **1992**, *63*, 271–277.

(20) Liu, Y.; Adronov, A. *Macromolecules* **2004**, *37*, 4755–4760.

Scheme 2

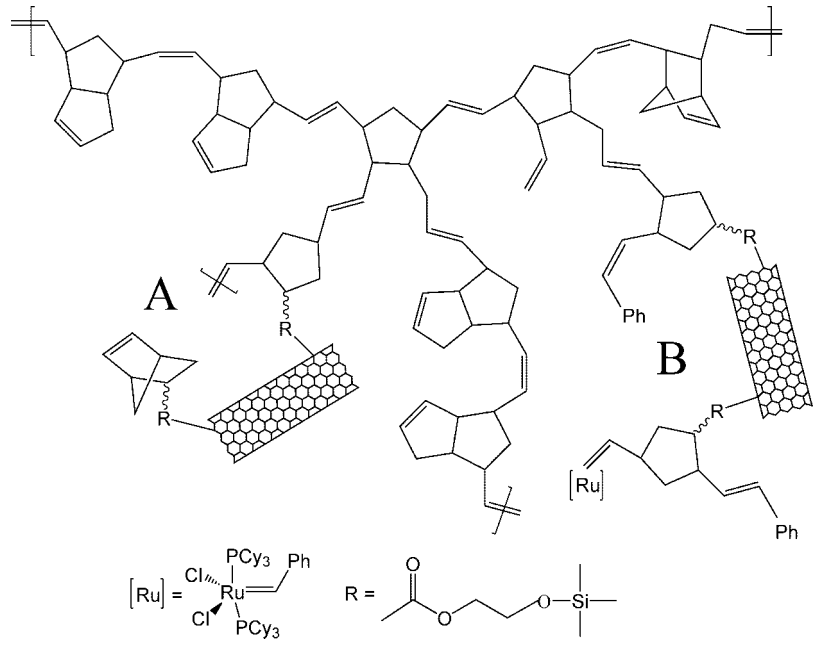

linear fashion from 2.44 to 25 MPa (Figure 7). All mechanical properties tested are tabulated in Table 1.

The increased elongation of f-MWNT/polyDCPD nanocomposites could be due to several toughening mechanisms. First, carbon nanotubes have been shown to toughen composites by bridging crazes at the onset of matrix fracture.[21] Nanoparticles have also been known to increase fracture toughness through the formation of a large number of subcritical microcracks or microvoids and retard flaw coalescence into critical cracks,[22] and to promote crack bridging effects and subsequent yielding of interparticle matrix ligaments.[23,24] Second, the interactions between the f-MWNTs and polyDCPD (through covalent bonds) during ROMP (Scheme 2) result in an interfacial region with properties and morphology which is different from the bulk polyDCPD network. Because of the large surface to volume ratio of the nanoreinforcement, this polymer specific interfacial region can become a dominant phase within the composite and vastly influence its thermomechanical behavior.

As mentioned earlier there is little increase of modulus and strength due to the relatively low loading of f-MWNTs. Normally in order to maximize load transfer from matrix to fillers, the length of fillers should be several times longer than a critical length;[3] however, nanotubes used in our experiment had broad length distributions with an average just below 2 μm (Figure 3c). The harsh oxidative process and repeated sonication during functionalization made the CVD-processed MWNTs undesirably short. Worse is that many submicrometer-length nanotubes are present, eliminating one of the key advantages of carbon nanotubes, high aspect ratio. The Halpin−Tsai model has been applied to predict the modulus of CNT-based polymer composites. There is a large variation in modulus for CVD-MWNTs reported in the literature with measured values ranging from 400 GPa[25] to just 50 GPa,[26] which means that the modulus strongly depends on the concentration of defects. As such, the experimental values for composite stiffness are compared with Halpin−Tsai predictions using two different moduli of CVD-MWNT: 400 and 50 GPa. For randomly oriented CNTs in a polymer matrix, the modulus of the composite is given by the following equation.

$$E_c = E_m\left[\frac{3}{8}\frac{1+2(l_{NT}/d_{NT})\eta_L v_{NT}}{1-\eta_T V_{NT}}+\frac{5}{8}\frac{1+2\eta_T V_{NT}}{1-\eta_T V_{NT}}\right]\eta_L = \frac{\left(\frac{E_{NT}}{E_M}\right)-1}{\left(\frac{E_{NT}}{E_M}\right)+2(l_{NT}/d_{NT})}\eta_T = \frac{\left(\frac{E_{NT}}{E_M}\right)-1}{\left(\frac{E_{NT}}{E_M}\right)+2} \quad (2)$$

where E_C, E_{NT}, and E_M represent the tensile modulus of the composite, carbon nanotubes, and the polymer matrix, respectively; l_{NT} is the length of the nanotubes, d_{NT} is their diameter, and V_{NT} is the volume fraction of nanotubes in the composite. The estimated values are $E_{NT} = 400$ GPa for E^a and $E_{NT} = 50$ GPa for E^b, $d_{NT} = 20$ nm, and $l_{NT} = 2$ μm. The experimental data fall between the two calculated values and show good agreement within the volume fraction range explored (Table 1).

To investigate how the norbornene grafted nanotubes influence the curing kinetics of DCPD, dynamic DSC scans for the DCPD and two different wt % of f-MWNTs with Grubbs' catalyst were performed (Figure 8). Dynamic scans show a small endothermic peak near 18 °C from the melting

(21) Qian, D.; Dickey, E. C.; rews, R.; Rantell, T. *Appl. Phys. Lett.* **2000**, *76*, 2868–2870.
(22) Wetzel, B.; Rosso, P.; Haupert, F.; Friedrich, K. *Eng. Fract. Mech.* **2006**, *73*, 2375–2398.
(23) Cardwell, B. J.; Yee, A. F. *J. Mater. Sci.* **1998**, *33*, 5473–5484.
(24) Lee, J.; Yee, A. F. *Polymer* **2001**, *42*, 589–597.
(25) Xie, S.; Li, W.; Pan, Z.; Chang, B; Sun, L. *J. Phys. Chem. Solids* **2000**, *61*, 1153–1158.
(26) Salvetat, J. P.; Kulik, A. J.; Bonard, J. M.; Briggs, A. D.; Stockli, T.; Metenier, K.; Bonnamy, S.; Beguin, F.; Burnham, N. A.; Forro, L. *Adv. Mater.* **1999**, *11*, 161–165.

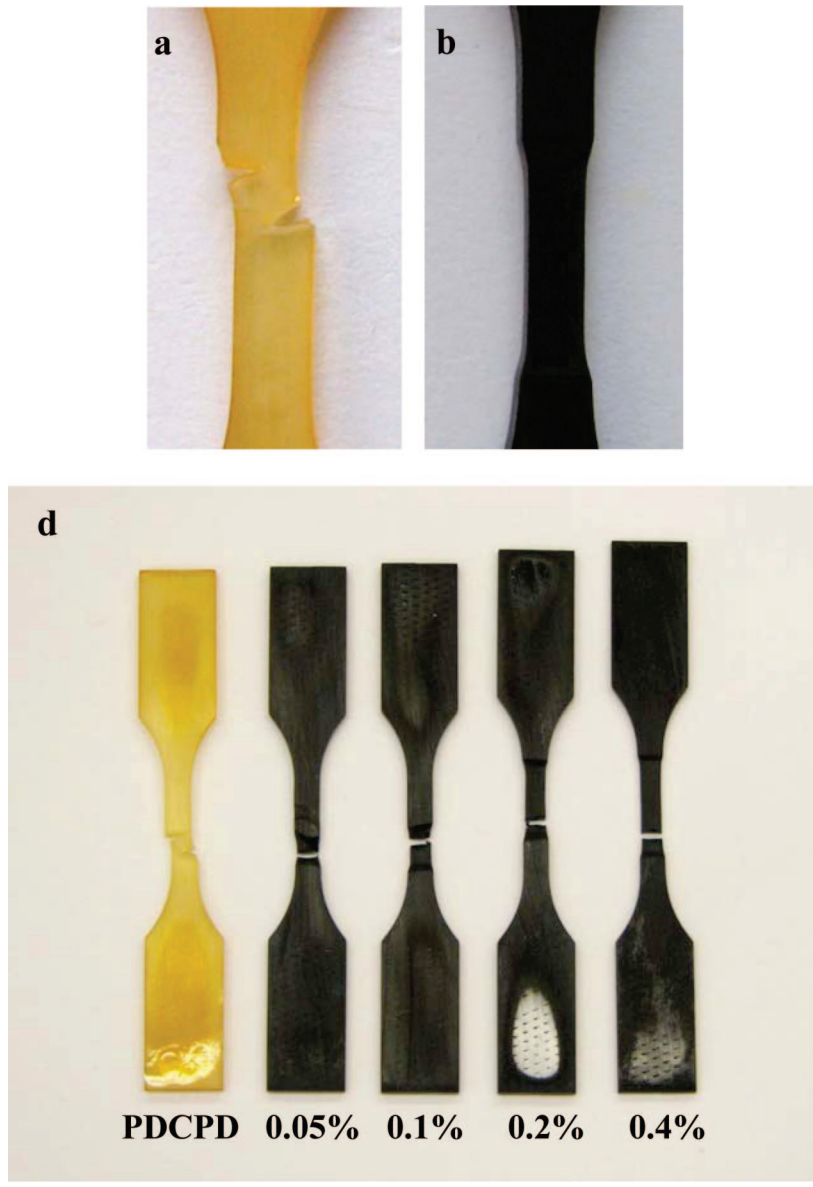

Figure 6. (a) Fractured morphology of brittle polyDCPD. (b) Reduction in gauge region during tension loadings of 0.4 wt % functionalized MWNT/polyDCPD composite. (c) Morphological change in the length of elongated sample with gauge length and fractured shape.

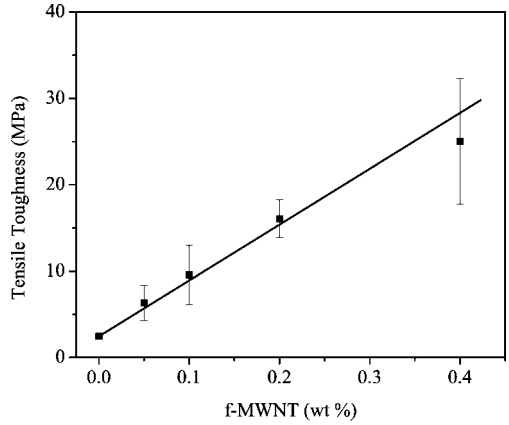

Figure 7. Changes in tensile toughness with respect to functionalized MWNT loadings.

of DCPD followed by a rapid exothermic peak corresponding to the ROMP of the DCPD monomer and the resulting relief of ring strain energy initiated by the highly reactive Grubbs' catalyst. It can be seen that there are distinct differences between the neat DCPD monomer and the samples with added f-MWNTs. For example, endothermic melting peaks gradually decrease from 18.5 to 15.8 °C with increasing nanotube loadings. Temperature scans of f-MWNT/DCPD solution without Grubbs' catalyst (not shown) similarly exhibit decreasing melting points with increasing nanotube loading. The exothermic peaks shifted to higher temperature from 59.40 to 60.93 to 62.80 °C (for 0, 0.2, and 0.4 wt % respectively), indicating a slightly slower reaction rate with increasing nanotube loading. Furthermore, the peak heights also decreased and the reaction heats gradually decreased from 375.5 to 371.7 to 368.0 J/g. However, the overall effect of f-MWNTs on the cure behavior of the DCPD is relatively minor.

The thermal and viscoelastic properties of the nanocomposites have been investigated by DMA. These tests were performed in order to evaluate the influence of norbornene f-MWNT on the thermal and viscoelastic properties of the

Table 1. Summary of Tensile Test Results for f-MWNT/polyDCPD Composite

		E^* (GPa)[a]					
	E (GPa)	E^a	E^b	σ (MPa)	ε_B (%)	toughness (MPa)	toughness change (%)
polyDCPD	2.07 ± 0.026	2.07	2.07	62.9 ± 1.28	5.75 ± 0.06	2.44 ± 0.05	
+ 0.05 wt% MWNT	2.09 ± 0.015	2.09	2.07	63.9 ± 0.89	13.3 ± 4.36	6.31 ± 2.05	158.6
+ 0.1 wt% MWNT	2.11 ± 0.057	2.10	2.08	64.9 ± 1.23	19.5 ± 5.96	9.55 ± 3.46	291.4
+ 0.2 wt% MWNT	2.12 ± 0.073	2.14	2.08	65.1 ± 2.12	33.7 ± 4.41	16.1 ± 2.18	558.3
+ 0.4 wt% MWNT	2.14 ± 0.026	2.21	2.10	65.3 ± 1.03	51.8 ± 15.2	25.0 ± 7.27	925.9

[a] E^*, Young's modulus calculated by Halpin−Tsai equation.

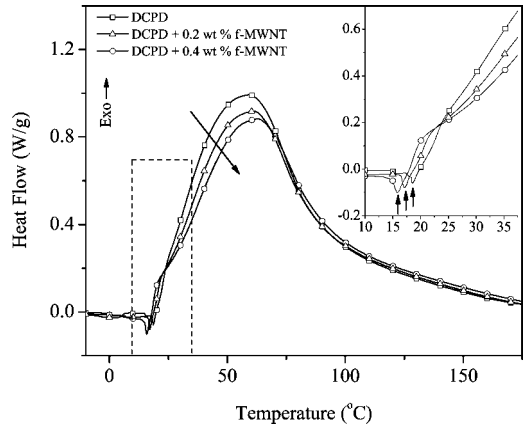

Figure 8. Differential scanning calorimetry dynamic scans at 10 °C/min.

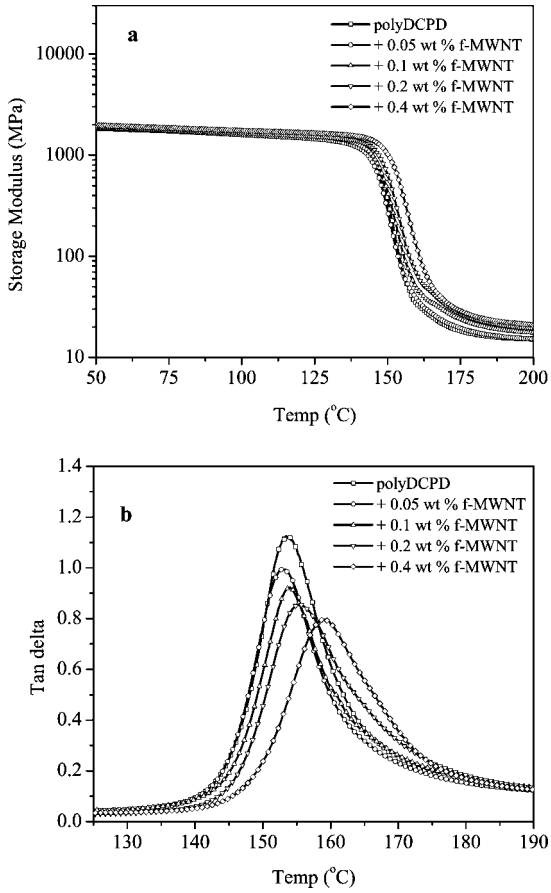

Figure 9. Dynamic mechanical analysis of functionalized MWNT/poyDCPD composite: (a) storage modulus (E'), (b) tan δ.

nanocomposites. Figure 9 shows the representative curves for storage modulus and tan delta as a function of temperature. As expected from tensile tests, the dynamic storage modulus only increases slightly in the glassy regions with increasing CNT loading. In general, the glass-transition temperature of nanocomposites depends on the interaction of nanofillers with the surrounding bulk polymer, increasing with attractive interactions (which yield wetted surfaces) and decreasing when effective free surfaces are formed.[27] In our sample, the addition of f-MWNTs shows a gradual increase of T_g (except the 0.05 wt % f-MWNT sample) and reduced damping of the composites. The T_g shifted from 153.85 to 159.15 °C for samples containing 0.4 wt % f-MWNTs. The increase of thermostability may be interpreted as a reduction of the mobility of the polyDCPD around the nanotubes by covalent bonds between f-MWNTs and the polyDCPD network. The magnitude of the tan delta peak decreases with increasing f-MWNT wt% (Figure 9b). If damping of the carbon nanotube is neglected (assuming perfectly elastic behavior) the effective interfacial thickness (ΔR) of the interphase between the CNTs and the polymer matrix can be estimated using the following equation:[28]

$$\tan \delta_c = \tan \delta_m \left(1 - \left(1 + \frac{\Delta R}{R}\right)^2 V_f\right) \quad (3)$$

where $\tan \delta_c$ is the damping of the composite, $\tan \delta_m$ is the damping of the matrix, V_f is the volume fraction of the functionalized nanotubes, and R is the radius of the nanotubes.

The calculated values are tabulated in Table 2. The effective interfacial thickness is about 200 nm at 0.1 wt %, which is 10 times thicker than the diameter of the nanotube. There is a general decreasing function of ΔR with respect to volume fraction, presumably indicating that as volume fraction increases, there is a greater chance that there is overlap between the interfacial thickness of adjacent nanotubes. Additionally, we can assume that at lower volume fractions, functionalized nanotubes are more ideally dispersed, and less likely to share interfacial volume.

Table 2. Summary of DMA Results for f-MWNT/polyDCPD Composite

	E' at (T_g + 30 °C) (MPa)	T_g (°C)	tan δ (peak height)	ΔR (nm)
polyDCPD	16.3	153.9	1.12	
+ 0.05 wt % MWNT	18.8	152.9	0.99	226.0
+ 0.1 wt % MWNT	19.9	154.0	0.92	199.2
+ 0.2 wt % MWNT	22.0	155.5	0.85	163.8
+ 0.4 wt % MWNT	22.4	159.2	0.81	124.5

(27) (a) Ash, B. J.; Schadler, L. S.; Siegel, R. W. *Mater. Lett.* **2002**, *55*, 83–87. (b) Rittigstein, P.; Torkelson, J. M. *J. Polym. Sci., Part B* **2006**, *44*, 2935–2943.
(28) (a) Vassileva, E.; Friedrich, K. *J. Appl. Polym. Sci.* **2003**, *89*, 3774–3785. (b) Iisaka, K.; Shibayama, K. *J. Appl. Polym. Sci.* **1977**, *22*, 3135–3143.

Conclusion

Nanocomposites consisting of low loadings of norbornene functionalized MWNTs and polyDCPD were developed. It was possible to achieve a homogeneous dispersion by grafting norbornene onto the nanotube surface. The investigation of mechanical properties of the nanocomposites resulted in a remarkable increase of tensile toughness (925% increase over the neat polyDCPD) with just 0.4 wt % functionalized MWNTs. Cure kinetics of composites show that there are slight decreases of melting point, exothermic heat, and reaction rate with increased nanotube loadings. DMA showed that there is a general increase in thermal stability (T_g) with the addition of functionalized nanotubes. Covalently bonded functionalized nanotubes reduce the mobility of the matrix by interfacial interactions resulting in a distinctive increase of glass transition temperature of the nanocomposites with nanotube loading. The dramatic effective interfacial thickness compared to the nanotube radius is additional evidence of strong interactions between the ROMP matrix and the nanotubes. Traditional methods for toughening thermosetting polymers with toughening agents typically come at the expense of other properties such as modulus, strength, or decreasing thermal stability. However, the system described here substantially increases the toughness, while at the same time increasing the modulus and glass-transition temperature using functionalized MWNTs via ROMP.

Acknowledgment. The authors thank J. C. DiCesare, W. K. Goertzen, X. Sheng, and T. C. Mauldin for their technical support and valuable discussions throughout the research and Prof. L. S. Chumbley for assistance in obtaining TEM images.

CM8020947